JACC: CARDIOVASCULAR IMAGING
VOL. 17, NO. 3, 2024

REVIEW

STATE-OF-THE-ART REVIEW

Ultrasound Shear Wave Elastography in Cardiology

Annette Caenen, PhD,[a,b,c,*] Stéphanie Bézy, MSc,[b,*] Mathieu Pernot, PhD,[d] Kathryn R. Nightingale, PhD,[e] Hendrik J. Vos, PhD,[c] Jens-Uwe Voigt, MD, PhD,[b,f] Patrick Segers, PhD,[a,†] Jan D'hooge, PhD[b,†]

ABSTRACT

The advent of high-frame rate imaging in ultrasound allowed the development of shear wave elastography as a noninvasive alternative for myocardial stiffness assessment. It measures mechanical waves propagating along the cardiac wall with speeds that are related to stiffness. The use of cardiac shear wave elastography in clinical studies is increasing, but a proper understanding of the different factors that affect wave propagation is required to correctly interpret results because of the heart's thin-walled geometry and intricate material properties. The aims of this review are to give an overview of the general concepts in cardiac shear wave elastography and to discuss in depth the effects of age, hemodynamic loading, cardiac morphology, fiber architecture, contractility, viscoelasticity, and system-dependent factors on the measurements, with a focus on clinical application. It also describes how these factors should be considered during acquisition, analysis, and reporting to ensure an accurate, robust, and reproducible measurement of the shear wave. (J Am Coll Cardiol Img 2024;17:314–329)

During the cardiac cycle, the stiffness of the myocardium changes because of the cyclic contraction and relaxation of its contractile elements. In a relaxed state, myocardial stiffness depends on the passive mechanical characteristics of the cardiomyocytes and the components of the extracellular matrix. Changes in myocardial stiffness may be found in many pathophysiological conditions affecting cardiac function. Assessing myocardial stiffness can therefore provide important clinical information for patient diagnosis and follow-up. Recent technological advancements in echocardiography have enabled high-frame rate imaging (typically 1,000 frames/s),[1] providing a gateway to a new, noninvasive tool for tissue stiffness assessment: shear wave elastography (SWE).[2] The high temporal resolution allows to study the propagation of externally or naturally induced mechanical shear waves (SWs) that travel along the cardiac wall. Interestingly, their propagation speed is linked to the stiffness of the tissue in which they propagate. Preclinical studies of cardiac SWE have demonstrated a clear relation between wave propagation speed and stiffness parameters derived from the end-diastolic pressure-volume relationship[3-5] and stress-strain relationship.[6,7] SWE has already been successfully implemented in clinical scanners for various noncardiac applications, such as the FibroScan (Echosens) for detecting liver fibrosis.

From the [a]Institute for Biomedical Engineering and Technology, Ghent University, Ghent, Belgium; [b]Department of Cardiovascular Sciences, University of Leuven, Leuven, Belgium; [c]Department of Cardiology, Erasmus MC University Medical Center, Rotterdam, the Netherlands; [d]Physics for Medicine, INSERM, CNRS, ESPCI, PSL University, Paris, France; [e]Department of Biomedical Engineering, Duke University, Durham, North Carolina, USA; and the [f]Department of Cardiovascular Diseases, University Hospitals Leuven, Leuven, Belgium. *Drs Caenen and Bézy contributed equally to this paper as joint first authors. †Drs Segers and D'hooge contributed equally to this paper as joint last authors.
The authors attest they are in compliance with human studies committees and animal welfare regulations of the authors' institutions and Food and Drug Administration guidelines, including patient consent where appropriate. For more information, visit the Author Center.

Manuscript received December 23, 2022; revised manuscript received November 14, 2023, accepted December 7, 2023.

ISSN 1936-878X/$36.00
https://doi.org/10.1016/j.jcmg.2023.12.007

In a previous review, Villemain et al[2] has summarized the increasing and encouraging evidence to support the potential clinical use of SWE in cardiac ultrasound, but its interpretation might be more complex. Indeed, the layered fiber structure of the myocardium makes the mechanical properties position- and direction-dependent, and the cyclic function of the heart leads to time- and loading-dependent changes. Additionally, factors related to the characteristics and configurations of the ultrasound system itself (system-dependent factors) also affect the relationship between wave propagation speed and myocardial stiffness. Therefore, in this paper we review the principles and clinical applications of cardiac SWE, but now with a particular focus on the appropriate interpretation of SW measurements in this challenging context, compared with the previous review of Villemain et al. Also, some recommendations are given on how to perform accurate and robust cardiac SWE measurements.

HOW TO DESCRIBE CARDIAC STIFFNESS?

MYOCARDIAL VS CHAMBER STIFFNESS. In the heart, stiffness can be measured as: 1) the intrinsic local material stiffness of the myocardium (ie, myocardial stiffness, as derived from stress-strain analysis);[8,9] and 2) the structural stiffness of a heart chamber as a whole (ie, chamber stiffness, as assessed using pressure-volume curves).[10] Chamber stiffness is not directly equivalent to myocardial stiffness, as it also depends on left ventricular (LV) morphology, muscle mass, and structures surrounding the LV. During systole, both chamber and myocardial stiffness are affected by myocyte contraction.[8]

STIFFNESS CONSTANT VS OPERATIONAL STIFFNESS. The mechanical behavior of the heart in diastole is commonly described by an exponential relation in a stress-strain or pressure-volume analysis. Two or more parameters, so-called stiffness constants, are generally necessary to mathematically describe this relation. The operational stiffness is defined as the slope of the tangent to these exponential relations at a given working point (Figure 1). Consequently, operational stiffness can vary because of either changes in preload for the same myocardium or changes of the myocardial stiffness constant at a certain loading state.

CARDIAC SWE

WHAT IS A SW AND HOW DOES IT RELATE TO TISSUE STIFFNESS? A SW is a type of mechanical wave in which an elastic material displaces perpendicular to the direction of wave propagation, as shown in Figure 2 (left). While the wave propagates, the material undergoes shearing, meaning that it changes shape without a change in volume, as illustrated in Figure 2 (right). As fluids cannot support shear forces, a SW cannot travel in fluids such as blood. The SW propagation speed (SWS) in elastic materials is directly linked to the stiffness constants of that material (ie, shear strength [expressed as shear modulus] that can be converted into the elasticity or Young's modulus when assuming tissue incompressibility)[11]:

$$v = \sqrt{\frac{\mu}{\rho}} \approx \sqrt{\frac{E/3}{\rho}} \quad (1)$$

with SWS v, shear modulus μ, elasticity modulus E, and mass density ρ (typically 1,000 kg/m^3). SWS in soft biological tissue is in the range of 0.5 to 20 m/s,[11] and pathologic changes can elevate its value up to 1 order of magnitude.[12]

ABBREVIATIONS AND ACRONYMS

ARF = acoustic radiation force
AVC = aortic valve closure
CA = cardiac amyloidosis
CMR = cardiac magnetic resonance
HCM = hypertrophic cardiomyopathy
HHD = hypertensive heart disease
LV = left ventricular
LVEDP = left ventricular end-diastolic pressure
MVC = mitral valve closure
PLAX = parasternal long-axis view
SWE = shear wave elastography
SWS = shear wave propagation speed

PRINCIPLES OF CARDIAC SWE. To date, 2 types of SWE have been applied to the heart in clinical studies, acoustic radiation force (ARF)-based SWE[13-17] and natural SWE,[18-20] as illustrated in Figure 3. The techniques differ in the manner of SW induction, but SW detection is realized with high-frame rate imaging in both cases:

- ARF-based SWE generates SWs using a localized ultrasound pulse with a pulse duration of 0.1 to 1 ms[21] that can be transmitted by a conventional

FIGURE 1 Illustrative Representation of End-Diastolic Pressure-Volume and Stress-Strain Relations

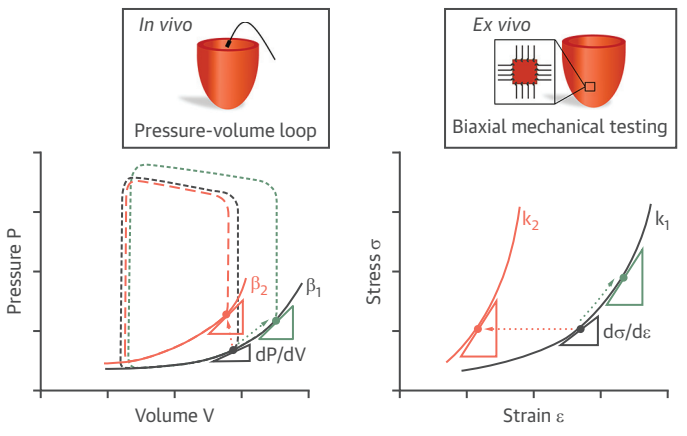

End-diastolic pressure-volume (left) and stress-strain (right) relations. Operating chamber stiffness (dP/dV) and operating myocardial stiffness (dσ/dε) can vary according to changes to loading (green triangle) or stiffness constants (red triangle).

JACC: CARDIOVASCULAR IMAGING, VOL. 17, NO. 3, 2024
MARCH 2024:314-329

FIGURE 2 A Shear Wave Displaces Perpendicular to the Direction of Wave Travel

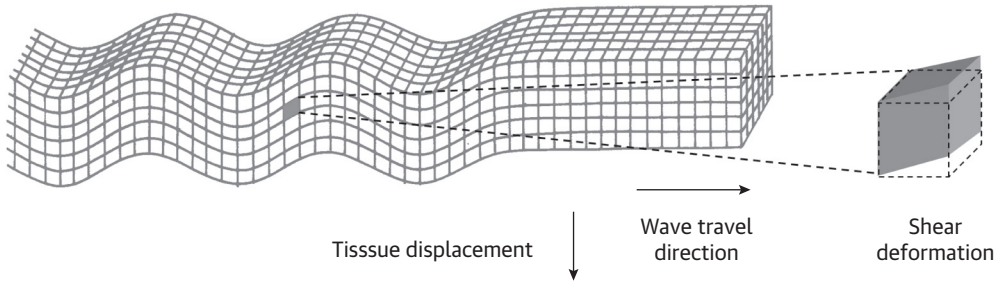

ultrasound transducer. This pulse locally pushes tissue away from the transducer (displacement magnitude of ~5 μm in the heart[15]) and is the origin of the SW propagation. An example of SW propagation in diastole and systole is illustrated in Figure 4.

- Natural SWE uses SWs caused by natural vibration sources of the heart (eg, mitral valve closure [MVC] and aortic valve closure [AVC]). When the valve closes, it causes an impact force on the basal region of the LV wall, generating a wave in the wall that propagates toward the apex with a displacement magnitude of about 100 μm.[18,22,23] An example of wave propagation after AVC is shown in Figure 5. As the wave source is less defined in terms of space, time, and magnitude, the exact wave nature

FIGURE 3 Principle of ARF-Based SWE and Natural SWE

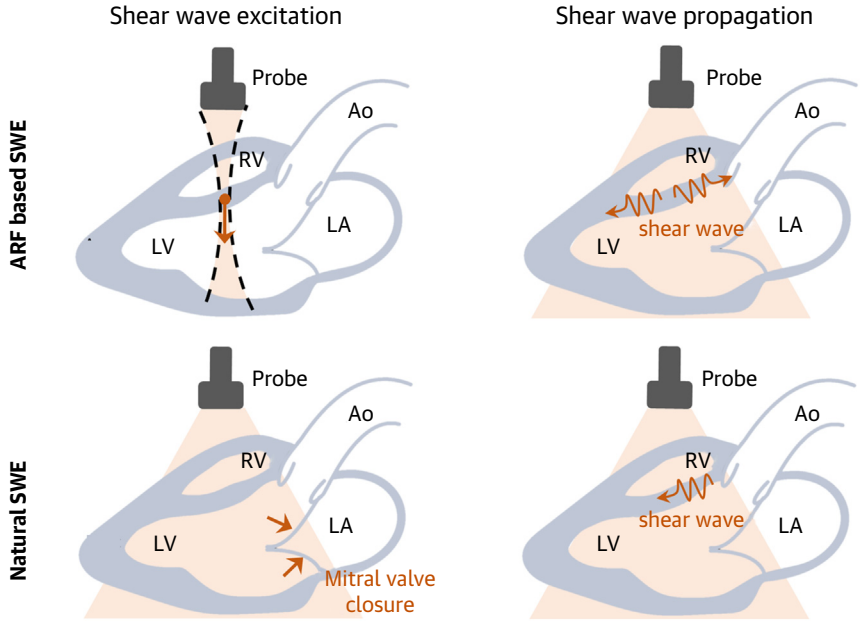

For acoustic radiation force (ARF)-based shear wave elastography (SWE), the probe first emits an impulsive ultrasound beam and consequently switches into high-frame rate imaging mode. The excited shear wave (SW) travels in a cylindrical fashion away from the push beam. For natural SWE, high-frame rate imaging is continuously used to visualize SW excitation and propagation. The SW is excited by physiological events such as mitral valve closure and travels from base to apex. Ao = aorta; LA = left atrium; LV = left ventricle; RV = right ventricle.

FIGURE 4 Example of ARF-Induced SW Propagation During Diastole and Systole in a Closed-Chest Pig

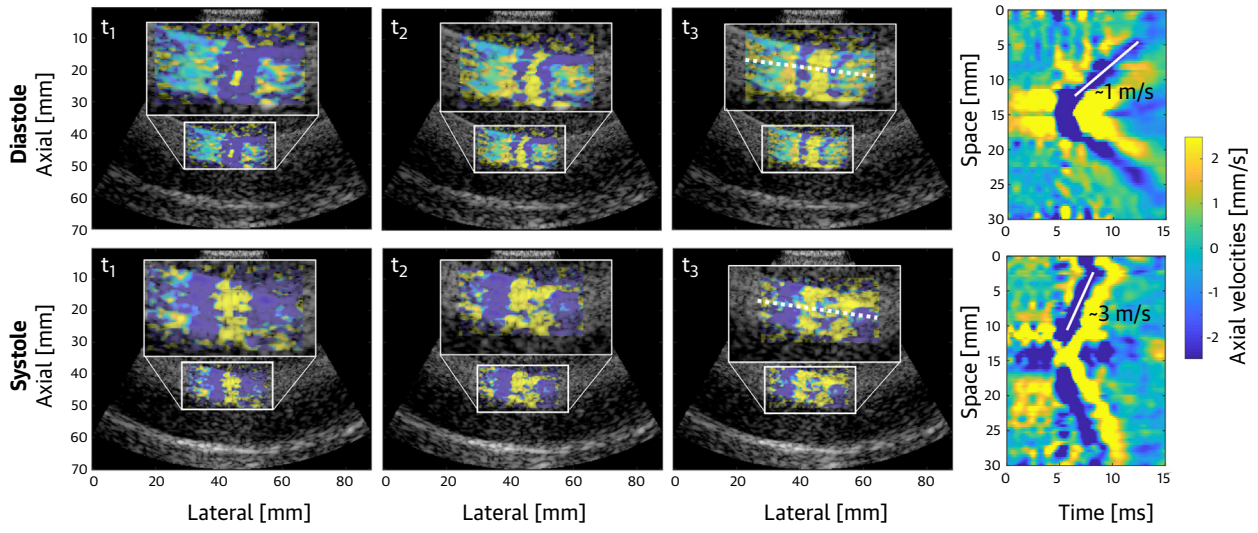

B-modes superimposed with tissue Doppler imaging in the parasternal long-axis view at 3 time points (left) and M-mode panels color-coded for tissue velocity representing the shear wave as a tilted color band with its slope indicating the propagation speed (right). M-mode is generated from the midinterventricular septum (white dotted line in third column). Details regarding the animal study can be found in the work by Caenen et al.[4] Abbreviations as in Figure 3.

and propagation direction may vary and are thus theoretically unknown.

SWs have been typically studied in the interventricular septum in the parasternal long-axis view (PLAX) using 2-dimensional (2D) high-frame rate imaging. Using tissue Doppler imaging techniques, the transverse component of wave motion is tracked during wave propagation along the wall, hence representing a "shear wave." Recent work[23] studied the natural wave propagation in 3 dimensions to determine the location of the wave excitation source(s) and the wave propagation direction in 3 volunteers (Figure 6), but optimization of the imaging sequence and postprocessing algorithms are necessary to apply it on a large scale.

SW motion is discriminated from gross cardiac tissue motion by applying a temporal filter,[19,24] subtracting average wall motion[6] or calculating tissue accelerations.[18] For SWS estimation, an anatomical

FIGURE 5 Example of Wave Propagation After AVC in a Healthy Volunteer

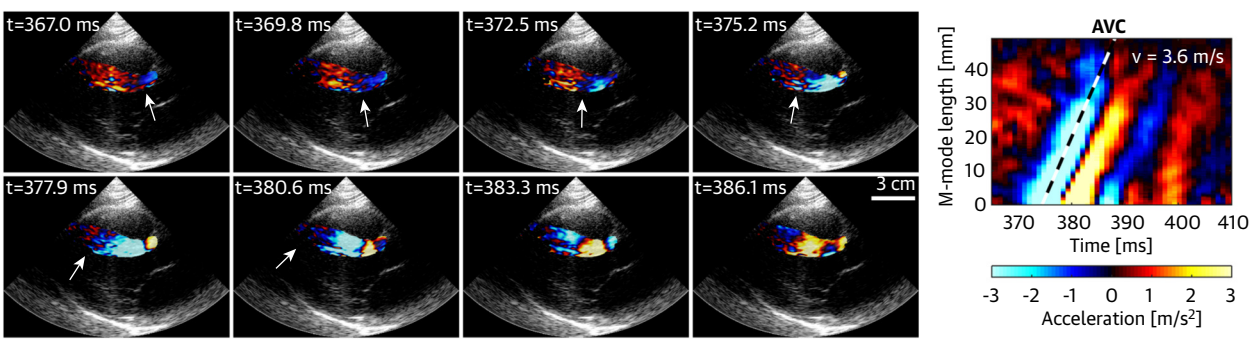

B-modes superimposed with tissue Doppler imaging in the parasternal long-axis view at 8 time points (left) and an M-mode panel color-coded for tissue acceleration representing the shear wave as a tilted color band with its slope indicating the propagation speed (right). Adapted with permission from Santos et al.[18] AVC = aortic valve closure.

FIGURE 6 Preliminary Results of 3-Dimensional High-Frame Rate Imaging Applied to the LV of 1 Healthy Volunteer in the Apical View

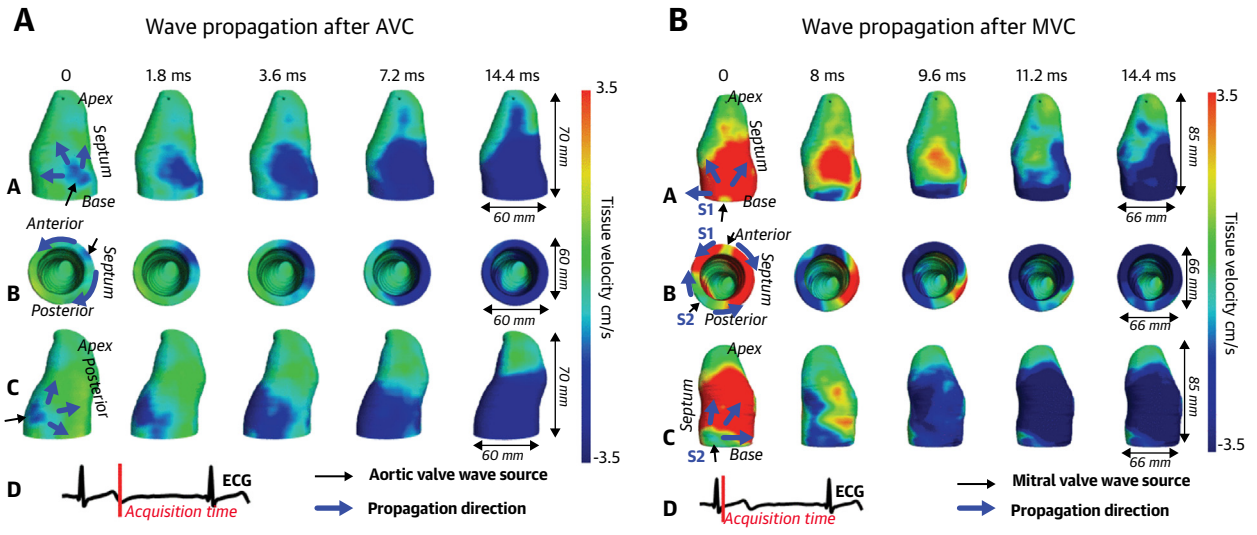

In A and B, row A represents the anterior wall view, row B the cross-sectional view from heart base, row C the posterior wall view, and row D the electrocardiogram (ECG) signal. (A) For the wave after AVC, the wave originated in the basal anteroseptum near the aortic valve and propagated from base to apex with an average speed of 3.4 m/s. The wave propagated faster from the septum to the posterior wall (5.4 ± 0.3 m/s) than from the septum to the anterior wall (3.5 ± 0.2 m/s). (B) For the wave after mitral valve closure (MVC), 2 wave sources were found near the base: one on the anteroseptal wall and a second on the posterior wall (S1 and S2), corresponding to the anchoring points of the mitral valve. The waves propagate along the anterior and posterior wall from base to apex with speeds of 2.8 ± 0.1 m/s along the long axis and 4.6 ± 0.3 m/s along the short axis for source S1 and 2.9 ± 0.2 m/s along the long axis for source S2. Adapted with permission from Papadacci et al.[23] Abbreviations as in Figures 3 and 5.

M-mode line is typically drawn along the midwall near the wave excitation source, representing the wave propagation path. The M-mode panel then displays the motion as a function of time (Figures 4 and 5), in which a propagating SW is displayed as a tilted color band of which the slope yields the SWS. When analyzing the wave pattern at 1 spatial location in the M-mode, Figure 7A shows that the number of crests and troughs depends on the selected quantity of tissue motion (displacement, velocity, or acceleration), and the first trough is typically tracked for wave speed estimation (Figures 4 and 5). Both tissue velocity and acceleration have been used in published research to visualize the SWs in cardiac SWE, and it is not clear yet which is superior to the other in terms of feasibility, accuracy, and robustness of wave speed estimation and diagnostics. Note that a 500-Hz recording of a SW traveling at 4 m/s along an M-mode line length of 4 cm gives 5 frames only to estimate the wave speed. Frame rates of 1,000 Hz or more are therefore preferred to precisely measure the speed of cardiac SWs in pathology.

Externally and naturally induced SWs are also studied using cardiac magnetic resonance (CMR), and we refer the reader to previous papers[25,26] for further details.

ARF-BASED SWE VS NATURAL SWE. The following differences in the characteristics of ARF-based and natural SWE affect their clinical applicability.

First, the measurement timing is different for both techniques. ARF-based SWE can be applied at any time point in the cardiac cycle to measure, eg, end-diastolic stiffness,[13,14] or it can be applied repetitively to measure dynamic stiffness variations[27-30] (Figure 8). Natural SW measurements occur after valve closures, which determine the onset of the isovolumic contraction or relaxation phase of the heart. They therefore represent not strictly end-diastolic or end-systolic stiffness.[29,31]

Second, measurement location is limited by how far the wave travels. For ARF-based SWE, SWs travel a short distance, requiring multiple acquisitions to assess stiffness at different locations. Furthermore, the technology is currently restricted to several LV wall segments in the PLAX and/or parasternal short-axis view,[15] because of technical limitations and the need for the ultrasound beam to be orthogonal with

FIGURE 7 Example of Tissue Motion Panels in 1 and 2 Dimensions (M-Mode) Depicting SW Propagation

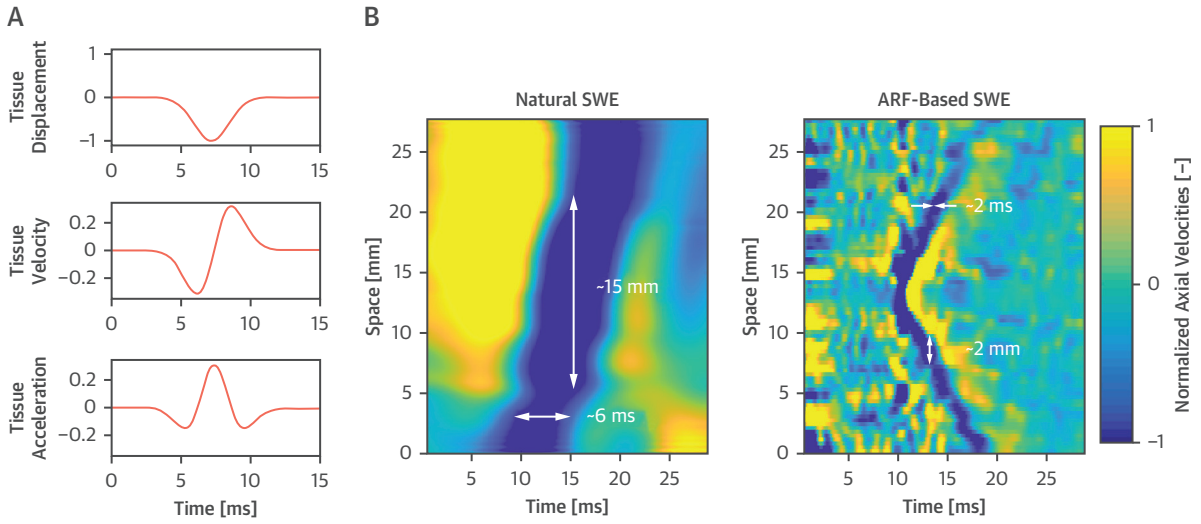

(A) Schematic representation of different tissue motion signals as a function of time in 1-dimensional space and (B) M-mode panels color-coded for tissue velocity, comparing natural and ARF-based SWE in in vivo pigs in the parasternal long-axis view. Abbreviations as in Figures 2 and 3.

the cardiac wall. In contrast, natural SWs travel farther and can span several myocardial segments.[23] Some studies[23,32,33] have used an apical view to record the longitudinal component of SW motion, similar to the FibroScan technology used in liver disease, but these propagation speeds cannot be directly compared with the propagation speed of the shear component in the PLAX view and showed higher variability.

Third, the wavelengths of natural waves in space and time are larger than those of ARF-induced waves (a few centimeters vs a few millimeters[29] and several milliseconds vs a few milliseconds) (Figure 7B), because of the differences in excitation source. The propagation speed of natural waves is therefore more susceptible to LV geometry and wall thickness, potentially influencing SWS.

Fourth, the feasibility of natural SWE is generally higher than that of ARF-based SWE,[16,18,29,33,34] as natural SWs have a higher amplitude and lower frequency content (less attenuation), resulting in a higher signal-to-noise ratio. Natural waves can therefore more easily be detected.

OTHER NATURAL MECHANICAL WAVES: ATRIAL KICK. Another type of natural wave that has been studied in the context of myocardial stiffness evaluation is the atrial kick wave, occurring after the P wave of the electrocardiographic signal in Figure 9.

FIGURE 8 Simultaneous ARF-Induced and Natural SWS Measurements in 1 Pig

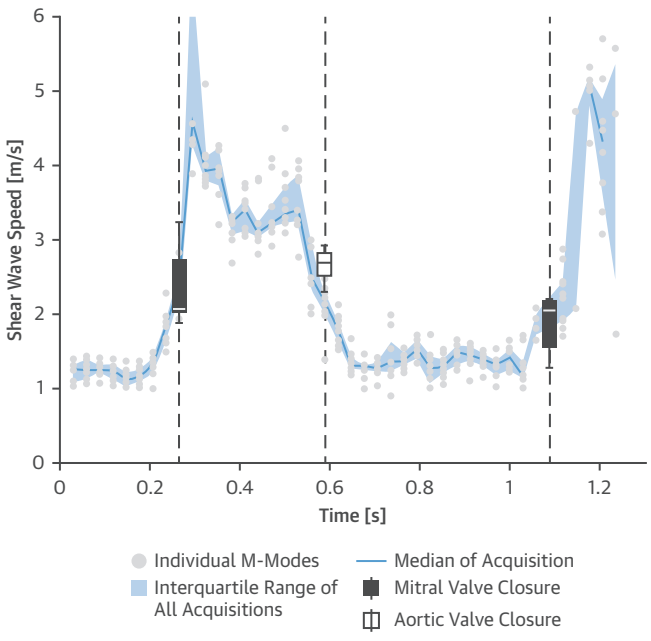

ARF-based shear wave speed (SWS) captures the dynamic stiffness variations during the cardiac cycle (gray spheres), whereas natural SWS (white and black boxplots) measures after aortic and mitral valve closure during the isovolumic phases of the cardiac cycle. Adapted with permission from Keijzer et al.[29] Abbreviation as in Figure 3.

FIGURE 9 M-Mode Color-Coded for Tissue Velocity Obtained From Clutter Filter Wave Imaging in Apical View, Depicting Propagation of Several Mechanical Waves Along the Septum Throughout the Cardiac Cycle in a Patient With Aortic Stenosis

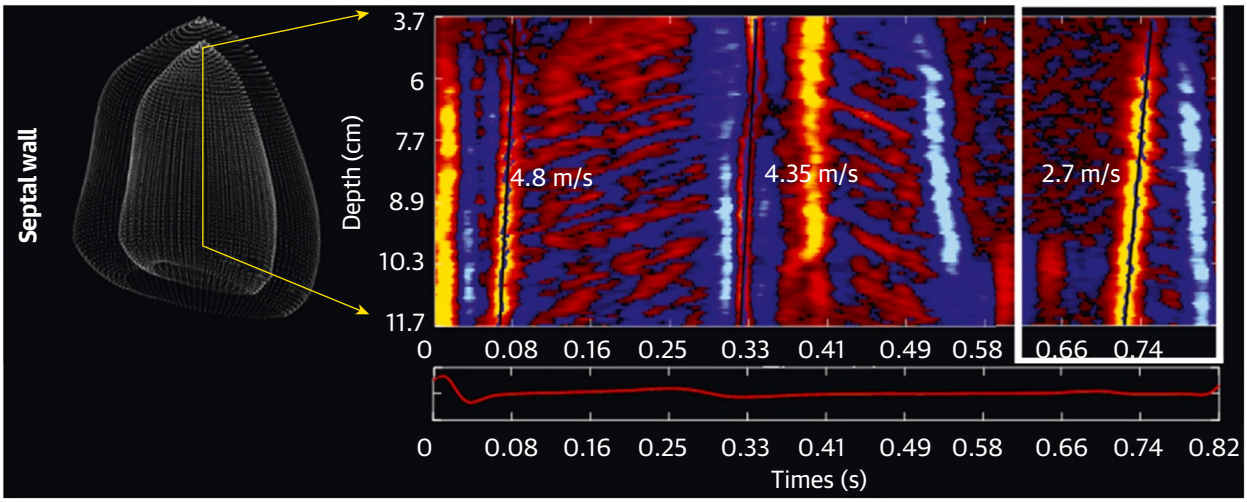

The atrial kick wave is highlighted with a white box and propagates with a speed of 2.7 m/s. The waves after mitral and aortic valve closure propagate with speeds of 4.8 and 4.35 m/s, respectively. Adapted with permission from Salles et al.[24]

An increased propagation speed of the atrial kick wave has been reported in patients with aortic stenosis,[24,33,35] cardiac amyloidosis (CA),[36] and hypertrophic cardiomyopathy (HCM),[37,38] as well as after preload increase in volunteers.[39] Its exact nature is not fully understood, but it is hypothesized to be a pressure wave resulting from the blood vortex traveling from the LV base to apex.[33,39] The atrial kick wave has been studied mainly in the apical view, although very recent work also used a parasternal view.[30,33] Its relation to myocardial stiffness is thus not given by equation 1 but by the theory of wave propagation in elastic tubes (the Moens-Korteweg equation),[35] analogous to pulse-wave velocity in arteries. As the atrial kick seems to have different mechanics from those assumed in SWE, in this review we do not further consider the atrial kick wave.

CLINICAL APPLICATION OF CARDIAC SWE

The initial feasibility and reproducibility of cardiac SWE have been investigated in several clinical studies, most often using experimental ultrasound systems and custom-built analysis software. A concise overview of reported SWS values in healthy subjects and different patient groups is provided in **Table 1**, and a full overview can be found in Supplemental Table 1. For healthy volunteers 20 to 40 years of age, ARF-based SWE yields a SWS of 1.6 m/s at end-diastole, whereas 3.1 and 3.5 m/s are measured for the natural waves after MVC and AVC, respectively. The difference in speeds between ARF-based and natural SWE is probably caused by the different timing in the cardiac cycle (**Figure 8**). All values increase with age, and significantly higher SWS has been reported for all SWE techniques in pathology, demonstrating the capability of SWE to distinguish healthy from diseased myocardium. Reported cutoff SWS values for various diseases are listed in **Table 2** (2.8 m/s for ARF-based SWE and 5.0 m/s for natural SWE on average). Examples of wave propagation after MVC are depicted in **Figure 10**, demonstrating how the wave propagation pattern is affected by disease, which leads to elevated SWS. The following sections discuss the application of SWE for assessing LV diastolic and systolic function.

SWE TO ASSESS LV DIASTOLIC FUNCTION. SWE can measure myocardial wall stiffness, a key determinant of diastolic dysfunction (Supplemental Table 2). End-diastolic ARF-induced SWS was related to CMR markers of fibrosis in patients with HCM[13]: 1) native T1 time; 2) T1 postcontrast; 3) extracellular volume fraction; and 4) late gadolinium enhancement. For natural SWE, SWSs after both MVC and AVC have been studied to assess myocardial stiffness. SWS after MVC correlated with CMR-defined diffuse myocardial injury in heart transplantation patients,[40] and its magnitude provided information on the degree of

remodeling in patients with hypertensive heart disease (HHD).[41] SWS after AVC showed a weak positive (nonsignificant) association with native T1 in a population consisting mainly of healthy volunteers.[33] It remains to be further investigated which natural wave is most suitable for myocardial stiffness estimation. The aforementioned research showed that SWE can detect fibrosis as a result of a long-term remodeling process, but SWE has also shown added value in detecting stiffening caused by an acute injury such as myocardial infarction (8.3 ± 1.6 m/s vs 4.6 ± 1.1 m/s).[42]

Diastolic SWS also correlated with conventional echocardiographic parameters of diastolic function in several patient populations, as summarized in Supplemental Table 2. A strong relation between SWS and E/e′ ratio, a marker of LV filling pressures, has been found in patients with CA, HCM, and HHD,[13,34,40,41,43,44] regardless of the technique used. SWS also positively correlated with other echocardiographic markers of diastolic function such as transmitral inflow pattern (E/A ratio),[13] global longitudinal strain,[44] and left atrial dimensions.[13,40,41,45] Furthermore, SWS increased with the grade of diastolic dysfunction in patients with CA.[34]

Chronic high filling pressures, indirectly reflected by increased left atrial size, have been shown to be associated with increased SWS in patients with HCM and HHD.[13,41] More important, SWS after MVC correlated moderately with pulmonary capillary wedge pressure in heart transplantation patients[40] and strongly with LV end-diastolic pressure (LVEDP) in patients referred for diagnostic catheter examination.[46] A cutoff of 5.3 m/s for SWS could predict elevated LVEDP with sensitivity and specificity of 92% and 89%, respectively[46] (Table 3).

SWE TO ASSESS LV SYSTOLIC FUNCTION (PRELIMINARY). ARF-based SWS in systole and SWS after AVC have been shown to be related to LV systolic function in preclinical studies.[27,47,48] In preliminary human data, this correlation was also observed for SWS after AVC for increasing exercise levels of bicycle testing and for increasing dobutamine doses (correlation with single beat end-systolic elastance: $r = 0.64$; $P < 0.001$[49]). In cardiac disease, however, the relation might not be as straightforward. An unchanged systolic ARF-induced SWS was reported in pigs after infarct-reperfusion injury[4,7] and in patients with HCM,[30] while increased SWS after AVC was seen in patients with CA[34] and HCM.[30,43] More clinical evidence with both SWE techniques in a large and diverse patient population is needed to further assess its role in systolic function evaluation.

TABLE 1 Overview of Reported SWS Values for Healthy Volunteers and Several Patient Groups in the Parasternal Long-Axis View

	ARF-Based SWE	Natural SWE	
	End-Diastole, m/s	MVC, m/s	AVC, m/s
Healthy volunteers (20-39 y)	1.6 ± 0.2[13,a]	3.1 ± 0.5[34]	3.5 ± 0.7[34]
Healthy volunteers (40-59 y)	2.2 ± 0.2[13,a]	3.8 ± 0.8[34]	3.8 ± 0.8[34]
Healthy volunteers (60-80 y)	2.4 ± 0.2[13,a]	4.5 ± 1.1[34]	4.3 ± 0.6[34]
Cardiac amyloidosis	NA	6.3 ± 1.6[34]	5.6 ± 1.1[34,44]
Hypertrophic cardiomyopathy	3.7 ± 0.3[13,a]	6.7 ± 1.3[43,b]	5.2 ± 0.8[43,b]
Hypertensive heart disease	NA	6.0 ± 1.4[41]	NA
Myocardial infarction	NA	7.9 ± 1.2[42]	NA
Heart transplantation	NA	5.7 ± 2.3[40]	NA
Aortic stenosis	NA	NA	3.4 ± 1.4[33,c]

As age is a confounding factor of wave speed estimation, patients of the same age group (60-80 y) were selected, unless stated otherwise. Although this age group was most common in all studies, additional data in younger populations is essential for SWE to serve as an early biomarker of cardiac stiffness. A more complete overview can be found in Supplemental Table 1. [a]Converted from shear stiffness by using equation 1 and assuming a density of 1,000 kg/m^3. [b]Mean patient age 51 ± 12 years. [c]Mean patient age 69 ± 12 years.

ARF = acoustic radiation force; AVC = aortic valve closure; MVC = mitral valve closure; NA = not available; SWE = shear wave elastography; SWS = shear wave propagation speed.

INTERPRETATION OF SW MEASUREMENTS

The relationship between SWS and myocardial stiffness is more complex than in equation 1, which is valid only for a large, isotropic material sample with a linear stress-strain relation. Hardly any of these

TABLE 2 Reported Cutoff Values of SWS for Various Populations, Together With Their Sensitivity, Specificity, and AUC

Population	First Author	Discriminating Factor	Excitation Source	AUC	Sensitivity, %	Specificity, %	Cutoff Speed, m/s
Hypertrophic cardiomyopathy	Villemain et al[13]	Normal vs cardiomyopathy	ARF[a]	0.99	95	100	2.8[b]
	Strachinaru et al[43]	Normal vs cardiomyopathy	AVC	0.98	95	90	4.0
Hypertensive heart disease	Cvijic et al[41]	Normal vs cardiomyopathy	MVC	0.97	94	91	4.99
Heart transplantation	Petrescu et al[40]	Normal vs elevated filling pressures	MVC	0.81	82	82	4.84
		Normal vs fibrosis	MVC	0.72	71	84	5.14
Patients with indication for heart catheterization	Werner et al[46]	Normal vs elevated filling pressures	MVC	0.94	92	89	5.3

[a]ARF was applied at end-diastole. [b]Converted from shear stiffness using equation 1 and assuming a density of 1,000 kg/m^3.

AUC = area under the curve; other abbreviations as in Table 1.

FIGURE 10 M-Mode Color-Coded for Tissue Acceleration Depicting the SW After Mitral Valve Closure in a Healthy Volunteer and Patients With Arterial Hypertension, Cardiac Amyloidosis and Hypertrophic Cardiomyopathy, Together With the ECG Signal

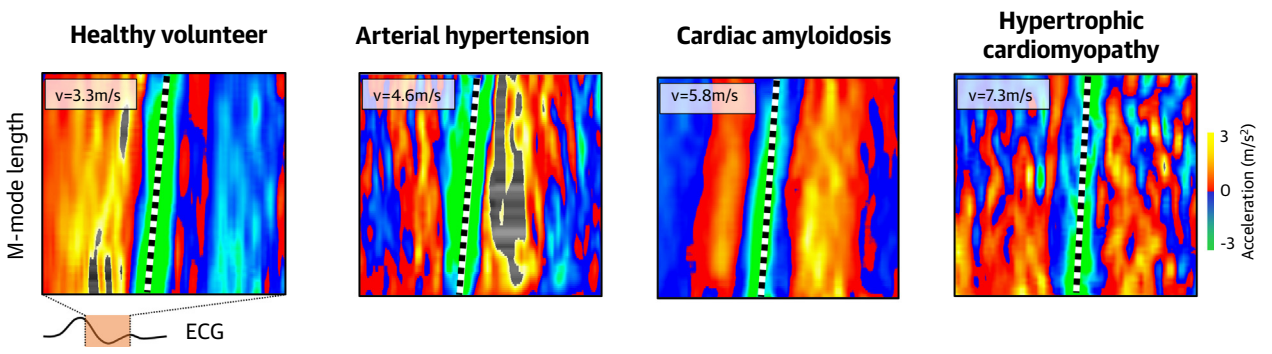

Wave speed is higher for patients than volunteers. ECG = electrocardiogram; SW = shear wave.

assumptions apply to the heart, whose tissue has a certain thickness (geometric boundaries) and is composed of layers with fibers of varying orientation (anisotropy) and in which operational stiffness depends on loading (material nonlinearity) and time (viscoelasticity, cyclic contraction). Furthermore, the relation between SWS and myocardial stiffness is also affected by the patient's age, determining the

TABLE 3 Overview of Factors Affecting SWS, Together With Descriptions of Their Effects, the Reported Variables That Correlated With SWS, and Our Suggestions on How to Account for Them

Factor Affecting Shear Wave Speed	Description of Effect	Reported Variable That Correlated With SWS	Authors' Suggestions to Account for Factor
Age	$SWS_{ARF,MVC,AVC}$ ↑ when age ↑	• Age[13,34,45]	• Create lookup tables of reference and cutoff speeds for different age groups/diseases
Ventricular loading	$SWS_{ARF,MVC,AVC}$ ↑ when preload/afterload ↑	• Invasive pressure measurements[40,46] • E/e′ ratio[13,34,40,41,43,44] • LA size: LA length,[45] LA diameter,[41] LAVI[13,40]	• Measure extra parameter (eg, wall stress or LV volume) • Perform extra SWE measurement at a loading change (eg, leg lifting or tilt-table test)[5] • Measure the transmural SWS gradient[51]
Ventricular morphology	$SWS_{ARF,MVC,AVC}$ ↑ when thickness ↑	• IVS thickness at end-diastole[41,44,45] • LV mass index[41,44]	• Report ventricular dimensions (eg, curvature, thickness) • Use frequency analysis to report main excited frequency of the wave and local dispersion slope
Viscoelasticity	$SWS_{ARF,MVC,AVC}$ ↑ when viscosity ↑[7,20,22,55,56]	• Heart rate[27] (no correlation reported but trend was shown)	• Use frequency analysis to report main excited frequency of the wave and local dispersion slope
Fiber architecture	$SWS_{ARF,MVC,AVC}$ ↑ when measuring along the fiber[13,23]	• Fiber tracking with diffusion tensor CMR[59]	• Perform SWE measurements in multiple echocardiographic views (or 3D SWE imaging) and report the wall segment analyzed
Contractility	$SWS_{ARF,MVC,AVC}$ affected by contraction[29] $SWS_{ARF,MVC,AVC}$ ↑ when contractility ↑[5,27,48,49]	• Invasive PV-based measures of contractility[5,27,48,49]	• Use ARF-based SWE imaging and time that to the diastolic phase when not interested in a measure of contractility
SWE settings	$SWS_{ARF,MVC,AVC}$ vary	NA	• Standardize SWE software in ultrasound systems concerning acquisition and analysis, and provide protocols • Define different cutoff speeds for natural and ARF-based SWE studies

3D = 3-dimensional; CMR = cardiac magnetic resonance; E/e′ = ratio of early mitral inflow velocity to mitral annular early diastolic velocity; IVS = interventricular septal; LA = left atrial; LAVI = left atrial volume index; LV = left ventricle; PV = pressure-volume; other abbreviations as in Table 1.

CENTRAL ILLUSTRATION Factors Other Than Myocardial Stiffness Affecting SWS

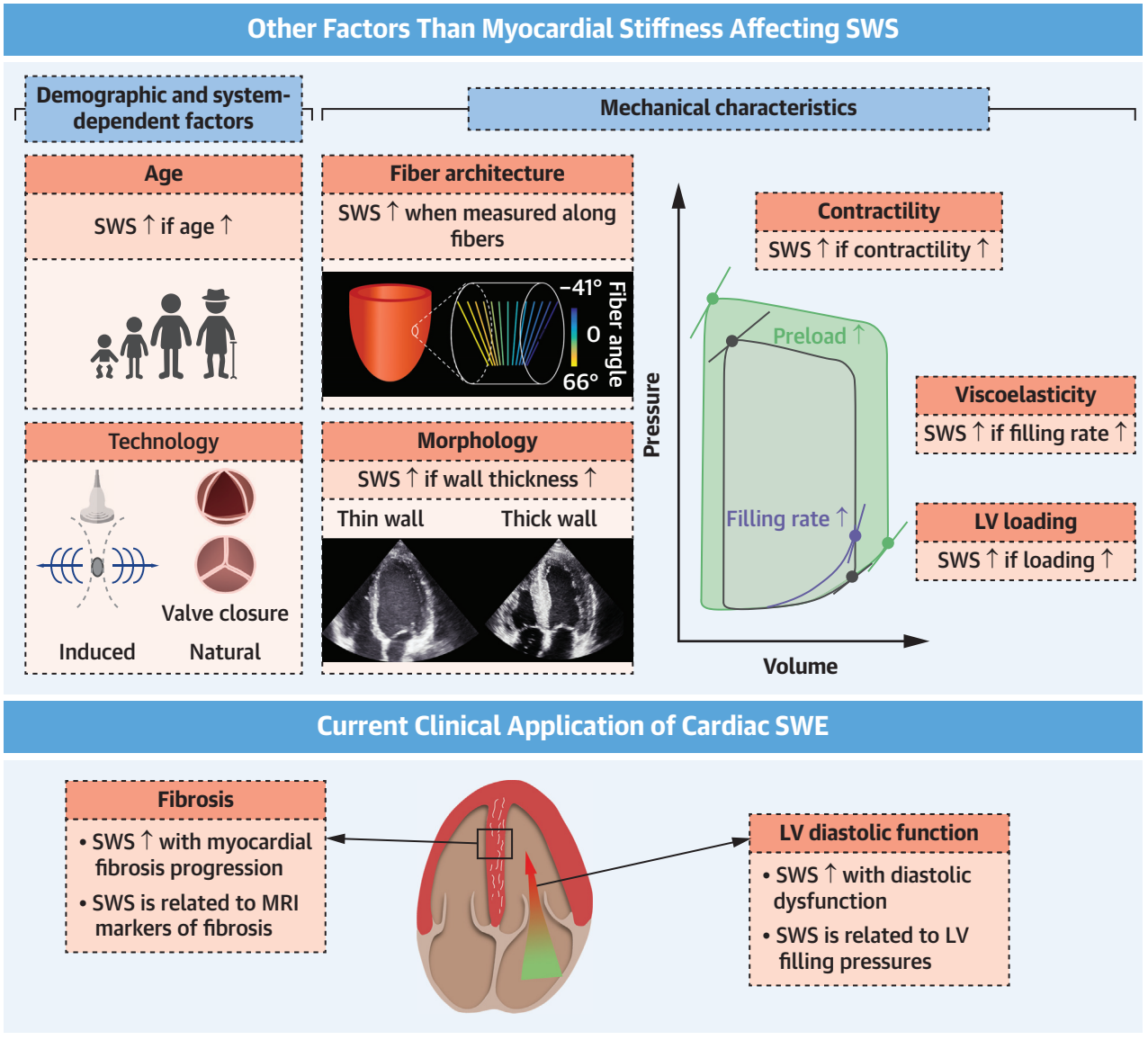

Caenen A, et al. J Am Coll Cardiol Img. 2024;17(3):314–329.

Factors other than myocardial stiffness that affect shear wave propagation speed (SWS) on shear wave elastography (SWE): age, fiber architecture, contractility, viscoelasticity, hemodynamic loading, morphology, system-dependent settings, and pathology. Typical findings are schematically shown for each factor. SWS increases have been reported in various patient populations with myocardial fibrosis and left ventricular (LV) diastolic dysfunction. CMR = cardiac magnetic resonance.

composition of the extracellular matrix and thus stiffness, and system-dependent factors. These influencing factors are summarized in **Table 3** (a complete overview is provided in Supplemental Table 2) and illustrated in the **Central Illustration**. Note that the effect size of a factor can be different for natural and ARF-based SWE, not only because of intrinsic differences but also because of pathologically altered valve closure affecting wave excitation in natural SWE.

AGE. For ARF-based SWE in diastole, SWS correlated with age in healthy volunteers: $r = 0.88$ for 20 to 80 years of age[13] and $r = 0.83$ for 0 to 45 years of age.[45] For natural SWE, healthy volunteers 60 to 80 years of age yielded higher speeds compared with those 20 to

FIGURE 11 Schematic Representation of SW Dispersion

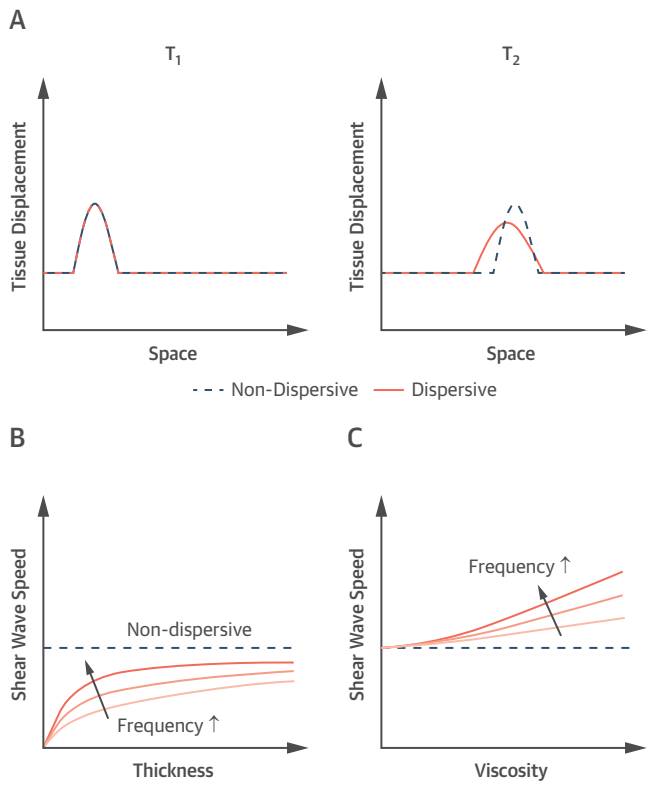

(A) SW propagation in dispersive and nondispersive media at 2 time points T_1 and T_2. (B, C) SW speed as a function of wall thickness (B) or viscosity (C) for nondispersive and dispersive media, while changing frequency. Abbreviation as in Figure 2.

39 years of age.[34] This agrees with the observed reduction of LV compliance due to aging.[50] Nomograms showing age-related normal values could help discriminate between normality and disease.

VENTRICULAR LOADING. An altered loading state of the LV due to changes in preload or afterload shifts the working point along the nonlinear stress-strain relation, affecting operational stiffness and thus SWS (**Figure 1**, **Central Illustration**). This has been confirmed in: 1) preclinical studies showing increased SWS after saline infusion and/or balloon inflation;[4,5,7,27] and 2) clinical studies demonstrating correlations between SWS and parameters reflecting filling pressures, such as E/e′ ratio,[13,34,41,43,44] pulmonary capillary wedge pressure,[40] and LVEDP[46] (Supplemental Table 2). To distinguish intrinsic myocardial stiffening from load-induced changes in operational stiffness, some concepts have been proposed to decouple this relationship (registration of an additional parameter such as wall stress[41] or transmural SWS gradient assessment),[51] but they need further clinical validation.

CARDIAC MORPHOLOGY. Wall thickness and curvature can guide the wave propagating inside the cardiac wall,[52] resulting in wave dispersion. This interaction can visually distort the waveshape during propagation (**Figure 11A**) and results in a frequency-dependent wave speed. Following Horace Lamb's theory,[53] the wave speed is then underestimated, especially for low frequencies (ie, large temporal wavelength, as in natural SWE) and thin walls (ie, pediatric patients), as shown in **Figure 11B**. This implies that increased SWS might be attributed partly to the thickened walls. For example, Lamb's model predicts that 21% of the natural SWS increase in a patient with 15-mm wall thickness is due to the thicker wall compared with a healthy volunteer with a 10-mm-thick wall. Clinical studies have confirmed a positive correlation between SWS and measures of LV morphology (Supplemental Table 2): wall thickness ($r = 0.79$ in HHD,[41] $r = 0.68$ in CA,[44] and $r = 0.72$ in healthy volunteers)[45] and LV mass index ($r = 0.76$ in HHD[41] and $r = 0.49$ in CA).[44] However, in a multiple linear regression analysis for ARF-based SWE in healthy volunteers,[45] wall thickness remained in the equation only when it was <4.4 mm (neonates). Wall thickness should therefore be reported, or taken into account through a frequency analysis,[20] but the latter is often not achievable because of inadequate signal-to-noise ratio.

VISCOELASTICITY. In SWE, tissue viscoelasticity causes wave attenuation and dispersion,[54] leading to a frequency-dependent wave speed. **Figure 11C** demonstrates an overestimated diastolic speed when viscosity and/or frequency increases. For example, the model predicts an increase in diastolic speed by 35% for ARF-based SWE when doubling viscosity. Next to pathologically altered viscoelastic properties, elevated SWS in cardiac disease might also be attributed to an increased deformation rate (heart rate), making the viscoelastic material appear stiffer when subjected to faster stretching.[54] Indeed, a heart rate dependence of SWS has been shown in Langendorff rat hearts.[27] Despite preclinical evidence of myocardial viscoelasticity affecting SWS,[7,20,22,27,55,56] clinical studies have largely ignored this aspect. Potential clinical value in quantifying viscoelastic effects through frequency analysis has been investigated for SWE in the liver.[57,58] However, its diagnostic value for cardiac SWE needs further investigation.

FIBER ARCHITECTURE. As SWs travel faster along the fiber than across,[13,23,59] the wave propagation pattern becomes elliptical in the plane of the fiber.

FIGURE 12 Effect of Transmural Varying Fiber Orientation on SW Elastography in a LV Model

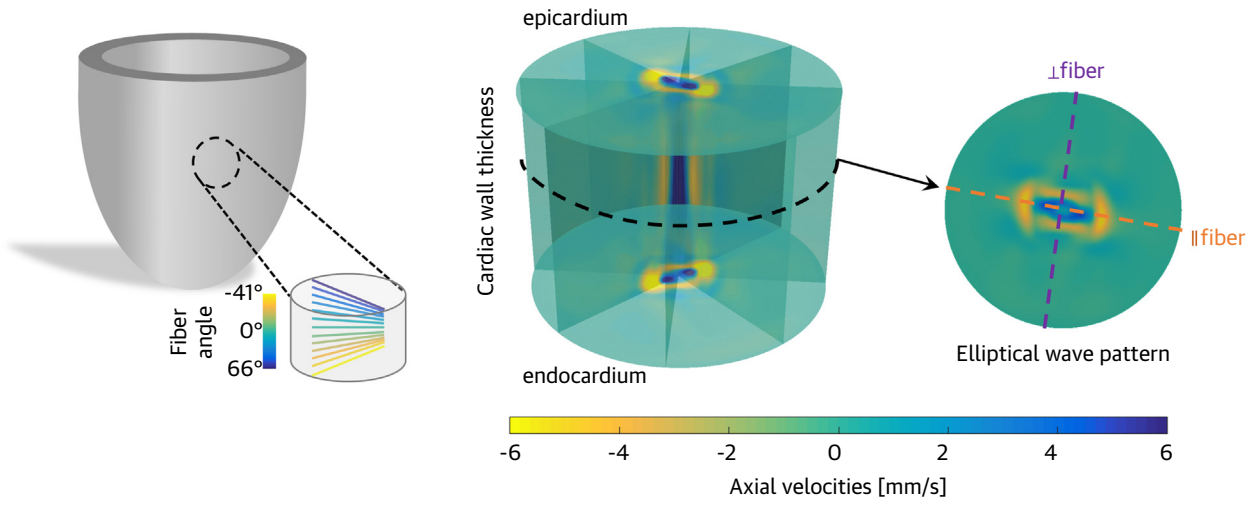

Simulated SW propagation is visualized in 3 dimensions at 1 time point (middle). The SW propagates faster along the fiber than across resulting in an elliptical wave profile (right). Abbreviations as in Figures 2 and 3.

The transmural varying fiber architecture of the heart will therefore generate complex 3-dimensional wave propagation patterns, as shown in Figure 12. This leads to a higher ARF-based SWS along the short axis compared with the long axis of the heart: 2.2 m/s vs 1.5 m/s in healthy volunteers. Such differences in speed are also found for natural SWE in the apical view[23] but need verification in a larger study. It is thus important to consistently consider the same view and wall depth in SWE. However, in case of fiber disarray, the difference in SWS might hold potential additional diagnostic value, and this concept forms the basis of a new parameter called fractional anisotropy. For more details on fractional anisotropy, we refer the reader to previous papers.[2,60]

CONTRACTILITY. SWS after AVC and ARF-based SWS in systole have been proposed as measures for contractility.[27,47,48] However, contractility might also affect SWS after MVC,[5,29,31] as the measurement occurs in the isovolumic contraction phase (Figure 8). Furthermore, in pigs receiving dobutamine, SWS after MVC significantly increased, although there was no relation with invasive global measures of LV contractility.[5] More research is needed to assess this effect in a large and diverse patient population.

SWE METHOD AND OTHER SYSTEM-DEPENDENT FACTORS. Intrinsic factors specific to the SWE-technique that affect SWS estimation are: 1) the unknown timing of natural SWE measurements with respect to the dynamics of cardiac muscle stiffness; 2) wave amplitude; and 3) wavelength (affecting SWS through wave dispersion, as discussed earlier). Other relevant factors are situated at the level of the measurement protocol (eg, echocardiographic view, number of measurements, outlier exclusion criteria) or at the postprocessing level (eg, clutter filters, wave speed estimator, analyzed type of tissue motion).[61,62] It is therefore essential to create standardized protocols for uniform data acquisition, analysis, and interpretation, as has been done for liver fibrosis staging using SWE.[63]

TOWARD CLINICAL TRANSLATION

BARRIERS TO THE IMPLEMENTATION OF SWE IN CLINICAL PRACTICE. Until now, cardiac SWE measurements are performed mainly with experimental ultrasound systems and custom-built analysis software. To investigate the diagnostic and prognostic power of SWE on a large scale for establishing reference and cutoff values, SWE needs to be integrated on clinical ultrasound systems of major vendors. Furthermore, to account for all confounding factors as discussed in this review, standardized protocols should be available for uniform data acquisition, analysis, reporting and interpretation. A starting point for this could be the suggestions formulated in Table 3 and Figure 13.

FIGURE 13 Recommendations for the Clinical Use of SW Measurements

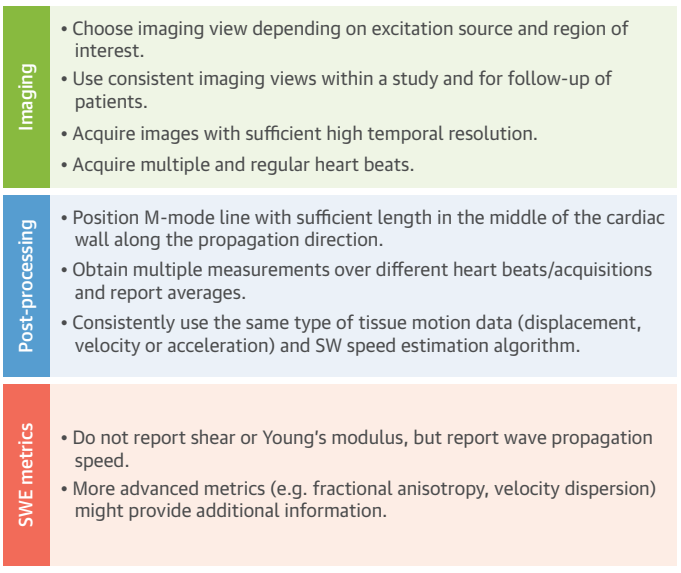

FA = fractional anisotropy; SW = shear wave; SWE = shear-wave elastography.

Concerning target patient populations, SWE measurements in the PLAX view have restricted current clinical studies to patients with septal pathology or with diffuse myocardial disease in which the septum is considered a representative sample. To expand the applicability to a wider range of patients, potential approaches include analyzing 2D SWE in multiple echocardiographic views[33] or using 3-dimensional imaging.[23] Other pressing issues include: 1) increasing the feasibility of stiffness evaluation throughout the cardiac cycle using ARF-based SWE, which is currently challenging[29,64] and reported only in a pediatric population;[30] and 2) assessing the appropriateness of wave speed after MVC for diastolic stiffness evaluation and wave speed after AVC for systolic stiffness evaluation.[29,65]

CLINICAL OUTLOOK FOR SWE. Cardiac SWE has shown to provide diagnostic information beyond conventionally evaluated parameters in patient populations with advanced cardiac dysfunction, but its sensitivity in detecting more subtle changes in cardiac function warrants further investigation. Longitudinal clinical trials are needed to assess the prognostic significance of SWE as well as its ability to improve outcomes by guiding patient management.

In the setting of multimodality imaging, cardiac SWE could have complementary value in patient diagnosis and prognosis, as it is currently the only available imaging modality providing noninvasive, direct, and quantitative measures of myocardial stiffness. Conventional echocardiography provides measures of diastolic function using cardiac volume, flow, and tissue velocity, and CMR provides information on the cause of diastolic dysfunction (presence of fibrosis), not tissue stiffness itself. Integrating SWE into clinical practice could enhance our understanding of the role of myocardial stiffness in pathophysiology, and in combination with other techniques, it will allow follow-up of therapy efficacy and a better patient stratification in the future. SWE might also have potential in systolic function evaluation, but this still needs to be further investigated.

RECOMMENDATIONS FOR THE CLINICAL USE OF CARDIAC SWE

To encourage consistency in data collection and reporting, this section proposes best practices in 2D cardiac SWE to provide guidance on how to obtain accurate and reproducible measurements. The main points are summarized in Figure 13 and are based on our previously published expert consensus statement.[66]

IMAGING. Typically, a PLAX view is used in SWE. Other (less common) echocardiographic views are the parasternal short-axis view for ARF-based SWE and apical 3- and 4-chamber views for natural SWE. Consistency in imaging view within a study and during patient follow-up is essential for: 1) studying the same wall; and 2) tracking the same component of tissue motion. During SWE acquisition, temporal resolution should be maximized, and an electrocardiographic trace should be simultaneously recorded to time the wave. Additional mitral and aortic valve Doppler spectra can be helpful for natural SWE. Obtaining multiple SWE measurements reduces the variability of the SWS estimates.

POSTPROCESSING. SWs can be visualized using a classical M-mode display, color-coded for tissue motion. The anatomical M-mode line represents the wave propagation path and is thus best positioned in the middle of the cardiac wall and parallel to the border, as transmural speed variations might be present.[51] It should be as long as possible, yet cover only the visible wave propagation path, to achieve accurate SWS estimates. The chosen wave speed estimator must be consistently used and clearly documented.

Analyzing and averaging multiple anatomical M-modes of different heartbeats or repeated acquisitions, especially in case of arrhythmias, will increase the robustness of the SWS estimates.

SWE-DERIVED METRICS. We recommend to report wave propagation speed as metric of SWE. Commercial noncardiac elastography systems convert speed into stiffness via equation 1, which relies on invalid material assumptions for the myocardium. Further insights can be gained from advanced metrics such as dispersion characteristics (how wave speed varies as a function of wave frequency) and fractional anisotropy (how wave speed is affected by the analyzed propagation direction). Reporting basic clinical information such as wall thickness, E/e′ ratio, and age is relevant for the correct interpretation of SWE.

CONCLUSIONS

More evidence is accumulating on the potential of cardiac SWE in improving patient diagnosis and prognosis, which will move SWE forward as a clinically useful tool for the noninvasive assessment of myocardial stiffness. Interpretation of SWE measurements is not straightforward, as they are affected by multiple factors from a mechanical point of view (eg, material nonlinearity, cardiac morphology) and a technical perspective (eg, echocardiographic view, tissue motion signal). Therefore, a continuing effort is needed to further validate SWE-derived parameters as markers of myocardial stiffness for different clinical scenarios and to standardize measurements for robust and reproducible application of cardiac SWE in the clinic.

HIGHLIGHTS

- SWE has potential to assess myocardial stiffness, providing insights into cardiac pathophysiology.
- Interpreting cardiac SW measurements requires a proper understanding of the SW physics.
- Technical/mechanical improvements and standardization will leverage SWE research into clinical reality.

FUNDING SUPPORT AND AUTHOR DISCLOSURES

This work was supported by the Research Foundation Flanders under grants 1211620N and 12B3124N to Dr Caenen and grant G092318N to Dr Bézy. Dr Voigt holds a personal research mandate of the Research Foundation Flanders (1832922N). Dr Nightingale has intellectual property related to radiation force-based imaging technologies that has been licensed to Siemens, Samsung, and MicroElastic Ultrasound Systems. Dr Pernot has intellectual property related to SWE that has been licensed to eMyoSound. Dr Vos has an ongoing research collaboration with Mindray Ultrasound. Drs Voigt and Jan D'hooge have an ongoing research collaboration with GE Vingmed. All other authors have reported that they have no relationships relevant to the contents of this paper to disclose.

ADDRESS FOR CORRESPONDENCE: Dr Jens-Uwe Voigt, Department of Cardiovascular Diseases, University Hospitals Leuven, Herestraat 49, 3000 Leuven, Belgium. E-mail: jens-uwe.voigt@uzleuven.be.

REFERENCES

1. Cikes M, Tong L, Sutherland GR, D'Hooge J. Ultrafast cardiac ultrasound imaging: technical principles, applications, and clinical benefits. *J Am Coll Cardiol Img*. 2014;7:812–823.

2. Villemain O, Baranger J, Friedberg MK, et al. Ultrafast ultrasound imaging in pediatric and adult cardiology: techniques, applications, and perspectives. *J Am Coll Cardiol Img*. 2020;13:1771–1791.

3. Vejdani-Jahromi M, Freedman J, Kim Y-J, Trahey GE, Wolf PD. Assessment of diastolic function using ultrasound elastography. *Ultrasound Med Biol*. 2018;44:551–561.

4. Caenen A, Keijzer L, Bézy S, et al. Continuous shear wave measurements for dynamic stiffness evaluation in pigs. *Sci Rep*. 2023;13(1):17660.

5. Bézy S, Duchenne J, Orlowska M, et al. Impact of loading and myocardial mechanical properties on natural shear waves. *J Am Coll Cardiol Img*. 2022;15:2024–2034.

6. Pernot M, Lee W-N, Bel A, et al. Shear wave imaging of passive diastolic myocardial stiffness: stunned vs infarcted myocardium. *J Am Coll Cardiol Img*. 2016;9:1023–1030.

7. Pislaru C, Urban MW, Pislaru SV, Kinnick RR, Greenleaf JF. Viscoelastic properties of normal and infarcted myocardium measured by a multi-frequency shear wave method: comparison with pressure-segment length method. *Ultrasound Med Biol*. 2014;40:1785–1795.

8. Villalobos Lizardi JC, Baranger J, Nguyen MB, et al. A guide for assessment of myocardial stiffness in health and disease. *Nat Cardiovasc Res*. 2022;1:8–22.

9. Guimarães CF, Gasperini L, Marques AP, Reis RL. The stiffness of living tissues and its implications for tissue engineering. *Nat Rev Mater*. 2020;5:351–370.

10. Burkhoff D, Mirsky I, Suga H. Assessment of systolic and diastolic ventricular properties via pressure-volume analysis: a guide for clinical, translational, and basic researchers. *Am J Physiol Heart Circ Physiol*. 2005;289:H501–H512.

11. Cobbold RSC. *Foundations of Biomedical Ultrasound*. New York: Oxford University Press; 2002.

12. Greenleaf JF, Fatemi M, Insana M. Selected methods for imaging elastic properties of biological tissues. *Annu Rev Biomed Eng*. 2003;5:57–78.

13. Villemain O, Correia M, Mousseaux E, et al. Myocardial stiffness evaluation using noninvasive shear wave imaging in healthy and hypertrophic cardiomyopathic adults. *J Am Coll Cardiol Img*. 2018;12:1135–1145.

14. Song P, Bi X, Mellema DC, et al. Pediatric cardiac shear wave elastography for quantitative assessment of myocardial stiffness: a pilot study in healthy controls. *Ultrasound Med Biol*. 2016;42:1719–1729.

15. Song P, Bi X, Mellema DC, et al. Quantitative assessment of left ventricular diastolic stiffness using cardiac shear wave elastography: a pilot study. *J Ultrasound Med*. 2016;35:1419–1427.

16. Correia M, Provost J, Chatelin S, Villemain O, Tanter M, Pernot M. Ultrafast harmonic coherent compound imaging for high frame rate echocardiography and shear wave elastography. *IEEE Trans Ultrason Ferroelectr Freq Control*. 2016;63:420–431.

17. Song P, Zhao H, Urban MW, et al. Improved shear wave motion detection using pulse-inversion harmonic imaging with phased array transducer. *IEEE Trans Med Imaging*. 2013;32:2299–2310.

18. Santos P, Petrescu A, Pedrosa J, et al. Natural shear wave imaging in the human heart: normal values, feasibility and reproducibility. *IEEE Trans Ultrason Ferroelectr Freq Control*. 2018;66:442–452.

19. Keijzer LBH, Strachinaru M, Bowen DJ, et al. Reproducibility of natural shear wave elastography measurements. *Ultrasound Med Biol*. 2019;45:3172–3185.

20. Kanai H. Propagation of spontaneously actuated pulsive vibration in human heart wall and in vivo viscoelasticity estimation. *IEEE Trans Ultrason Ferroelectr Freq Control*. 2005;52:1931–1942.

21. Nightingale K. Acoustic radiation force impulse (ARFI) imaging: a review. *Curr Med Imaging Rev*. 2011;7:328–339.

22. Vos HJ, van Dalen BM, Heinonen I, et al. Cardiac shear wave velocity detection in the porcine heart. *Ultrasound Med Biol*. 2017;43:753–764.

23. Papadacci C, Finel V, Villemain O, Tanter M, Pernot M. 4D ultrafast ultrasound imaging of naturally occurring shear waves in the human heart. *IEEE Trans Med Imaging*. 2020;39:4436–4444.

24. Salles S, Espeland T, Molares A, et al. 3D myocardial mechanical wave measurements. *J Am Coll Cardiol Img*. 2021;14(8):1495–1505.

25. Arani A, Arunachalam SP, Chang ICY, et al. Cardiac MR elastography for quantitative assessment of elevated myocardial stiffness in cardiac amyloidosis. *J Magn Reson Imaging*. 2017;46:1361–1367.

26. Troelstra MA, Runge JH, Burnhope E, et al. Shear wave cardiovascular MR elastography using intrinsic cardiac motion for transducer-free non-invasive evaluation of myocardial shear wave velocity. *Sci Rep*. 2021;11:1403.

27. Pernot M, Couade M, Mateo P, Crozatier B, Fischmeister R, Tanter M. Real-time assessment of myocardial contractility using shear wave imaging. *J Am Coll Cardiol*. 2011;58:65–72.

28. Couade M, Pernot M, Messas E, et al. In vivo quantitative mapping of myocardial stiffening and transmural anisotropy during the cardiac cycle. *IEEE Trans Med Imaging*. 2011;30:295–305.

29. Keijzer LBH, Caenen A, Voorneveld J, et al. A direct comparison of natural and acoustic-radiation-force-induced cardiac mechanical waves. *Sci Rep*. 2020;10(1):18431.

30. Malik A, Villalobos Lizardi JC, Baranger J, et al. Comparison between acoustic radiation force-induced and natural wave velocities for myocardial stiffness assessment in hypertrophic cardiomyopathy. *J Am Coll Cardiol Img*. 2024;17(2):223-225. https://doi.org/10.1016/j.jcmg.2023.07.015

31. Pernot M, Villemain O. In the heart of stiffness: are natural heart vibrations reliable enough to assess myocardial stiffness, the new holy grail in echocardiography? *J Am Coll Cardiol Img*. 2019;12:2399–2401.

32. Keijzer LBH, Strachinaru M, Bowen DJ, et al. Parasternal versus apical view in cardiac natural mechanical wave speed measurements. *IEEE Trans Ultrason Ferroelectr Freq Control*. 2020;67:1590–1602.

33. Espeland T, Wigen MS, Dalen H, et al. Mechanical wave velocities in left ventricular walls in healthy subjects and patients with aortic stenosis. *J Am Coll Cardiol Img*. 2024;17(2):111-124. https://doi.org/10.1016/j.jcmg.2023.07.009

34. Petrescu A, Santos P, Orlowska M, et al. Velocities of naturally occurring myocardial shear waves increase with age and in cardiac amyloidosis. *J Am Coll Cardiol Img*. 2019;12:2389–2398.

35. Pislaru C, Alashry MM, Thaden JJ, Pellikka PA, Enriquez-Sarano M, Pislaru SV. Intrinsic wave propagation of myocardial stretch, a new tool to evaluate myocardial stiffness: a pilot study in patients with aortic stenosis and mitral regurgitation. *J Am Soc Echocardiogr*. 2017;30:1070–1080.

36. Pislaru C, Ionescu F, Alashry M, et al. Myocardial stiffness by intrinsic cardiac elastography in patients with amyloidosis: comparison with chamber stiffness and global longitudinal strain. *J Am Soc Echocardiogr*. 2019;32:958–968.e4.

37. Strachinaru M, Geleijnse ML, de Jong N, et al. Myocardial stretch post-atrial contraction in healthy volunteers and hypertrophic cardiomyopathy patients. *Ultrasound Med Biol*. 2019;45:1987–1998.

38. Naser JA, Anupraiwan O, Adigun RO, et al. Myocardial stiffness by cardiac elastography in hypertrophic cardiomyopathy: relationship with myocardial fibrosis and clinical outcomes. *J Am Coll Cardiol Img*. 2021;14:2051–2053.

39. Voigt JU, Lindenmeier G, Werner D, et al. Strain rate imaging for the assessment of preload-dependent changes in regional left ventricular diastolic longitudinal function. *J Am Soc Echocardiogr*. 2002;15:13–19.

40. Petrescu A, Bézy S, Cvijic M, et al. Shear wave elastography using high-frame-rate imaging in the follow-up of heart transplantation recipients. *J Am Coll Cardiol Img*. 2020;13:2304–2313.

41. Cvijic M, Bézy S, Petrescu A, et al. Interplay of cardiac remodelling and myocardial stiffness in hypertensive heart disease: a shear wave imaging study using high-frame rate echocardiography. *Eur Heart J Cardiovasc Imaging*. 2020;21:664–672.

42. Wouters L, Duchenne J, Bézy S, et al. Septal scar detection in patients with left bundle branch block using echocardiographic shear wave elastography. *J Am Coll Cardiol Img*. 2023;16:713–715.

43. Strachinaru M, Bosch JG, van Gils L, et al. Naturally occurring shear waves in healthy volunteers and hypertrophic cardiomyopathy patients. *Ultrasound Med Biol*. 2019;45:1977–1986.

44. Jin FQ, Kakkad V, Bradway DP, et al. Evaluation of myocardial stiffness in cardiac amyloidosis using acoustic radiation force impulse and natural shear wave imaging. *Ultrasound Med Biol*. 2023;49(8):1719–1727.

45. Malik A, Baranger J, Nguyen MB, et al. Impact of ventricular geometric characteristics on myocardial stiffness assessment using shear-wave velocity in healthy children and young adults. *J Am Soc Echocardiogr*. 2023;36(8):849–857.

46. Werner AE, Bézy S, Orlowska M, et al. How well does SWE predict elevated filling pressures? A comparison to the current guideline algorithm. *Eur Heart J Cardiovasc Imaging*. 2022;23(suppl 1).

47. Vejdani-Jahromi M, Freedman J, Nagle M, Kim Y-J, Trahey GE, Wolf PD. Quantifying myocardial contractility changes using ultrasound-based shear wave elastography. *J Am Soc Echocardiogr*. 2017;30:90–96.

48. Bézy S, Caenen A, Duchenne J, Orlowska M, D'hooge J, Voigt J. Systolic shear wave propagation speed as a novel non-invasive marker of myocardial contractility. *Eur Heart J Cardiovasc Imaging*. 2022;23:jeab289.

49. Bézy S, Cvijic M, Petrescu A, et al. Shear wave propagation velocity after aortic valve closure could be a novel parameter for myocardial contractility. *Eur Heart J Cardiovasc Imaging*. 2020;21(suppl 1):jez319.034.

50. de Souza RR. Ageing of myocardial collagen. *Biogerontology*. 2002;3:325–335.

51. Caenen A, Bézy S, Petrescu A, et al. Transmural wave speed gradient may distinguish intrinsic myocardial stiffening from preload-induced changes in operational stiffness in shear wave elastography. *IEEE Trans Biomed Eng*. 2022;70(1):259–270.

52. Caenen A, Pernot M, Shcherbakova DA, et al. Investigating shear wave physics in a generic pediatric left ventricular model via in vitro experiments and finite element simulations. *IEEE Trans Ultrason Ferroelectr Freq Control*. 2017;64:349–361.

53. Rose JL. *Ultrasonic Guided Waves in Solid Media*. New York: Cambridge University Press; 2014.

54. Li H, Flé G, Bhatt M, et al. Viscoelasticity Imaging of biological tissues and single cells using shear wave propagation. *Front Phys*. 2021;9.

55. Urban MW, Pislaru C, Nenadic IZ, Kinnick RR, Greenleaf JF. Measurement of viscoelastic properties of in vivo swine myocardium using lamb wave dispersion ultrasound vibrometry (LDUV). *IEEE Trans Med Imaging*. 2013;32:247–261.

56. Nenadic IZ, Urban MW, Pislaru C, Escobar D, Vasconcelos L, Greenleaf JF. In vivo open- and closed-chest measurements of left-ventricular myocardial viscoelasticity using lamb wave

dispersion ultrasound vibrometry (LDUV): a feasibility study. *Biomed Phys Eng Express*. 2018;4.

57. Sugimoto K, Moriyasu F, Oshiro H, et al. Clinical utilization of shear wave dispersion imaging in diffuse liver disease. *Ultrasonography*. 2020;39:3–10.

58. Nightingale KR, Rouze NC, Rosenzweig SJ, et al. Derivation and analysis of viscoelastic properties in human liver: impact of frequency on fibrosis and steatosis staging. *IEEE Trans Ultrason Ferroelectr Freq Control*. 2015;62:165–175.

59. Lee WN, Larrat B, Pernot M, Tanter M. Ultrasound elastic tensor imaging: comparison with MR diffusion tensor imaging in the myocardium. *Phys Med Biol*. 2012;57:5075–5095.

60. Pedreira O, Correia M, Chatelin S, et al. Smart ultrasound device for non invasive real time myocardial stiffness quantification of the human heart. *IEEE Trans Biomed Eng*. 2021;69:42–52.

61. Rouze NC, Deng Y, Trutna CA, Palmeri ML, Nightingale KR. Characterization of viscoelastic materials using group shear wave speeds. *IEEE Trans Ultrason Ferroelectr Freq Control*. 2018;65:780–794.

62. Seliverstova E, Caenen A, Bézy S, Nooijens S, Voigt JU, D'Hooge J. Comparing myocardial shear wave propagation velocity estimation methods based on tissue displacement, velocity and acceleration data. *Ultrasound Med Biol*. 2022;48(11):2207–2216.

63. Palmeri ML, Milkowski A, Barr R, et al. Radiological Society of North America/Quantitative Imaging Biomarker Alliance shear wave speed bias quantification in elastic and viscoelastic phantoms. *J Ultrasound Med*. 2021;40:569–581.

64. Kakkad V, LeFevre M, Hollender P, Kisslo J, Trahey GE. Non-invasive measurement of dynamic myocardial stiffness using acoustic radiation force impulse imaging. *Ultrasound Med Biol*. 2019;45:1112–1130.

65. Villemain O, Pernot M. To be, or not to be diastolic: about natural mechanical waves after mitral valve closure. *J Am Coll Cardiol Img*. 2022;15:2035–2037.

66. Caenen A, Pernot M, Nightingale KR, et al. Assessing cardiac stiffness using ultrasound shear wave elastography. *Phys Med Biol*. 2022;67.

KEY WORDS cardiac function, echocardiography, myocardial stiffness, review, shear wave elastography

APPENDIX For supplemental tables and references, please see the online version of this paper.